Increasing trap stiffness with position clamping in holographic optical tweezers

Daryl Preece[1,†], Richard Bowman[1,†], Anna Linnenberger[2], Graham Gibson[1], Steven Serati[2] and Miles Padgett[1]

[1] *Department of Physics and Astronomy, SUPA, University of Glasgow, G12 8QQ, UK*
[2] *Boulder Nonlinear Systems, 450 Courtney Way, 107 Lafayette, CO 80026,USA*
[†] *These authors have contributed equally to this work.*
d.preece@physics.gla.ac.uk

http://www.physics.gla.ac.uk/Optics/

Abstract: We present a holographic optical tweezers system capable of position clamping multiple particles. Moving an optical trap in response to the trapped object's motion is a powerful technique for optical control and force measurement. We have now realised this experimentally using a Boulder Nonlinear Systems Spatial Light Modulator (SLM) with a refresh rate of 203Hz. We obtain a reduction of 44% in the variance of the bead's position, corresponding to an increase in effective trap stiffness of 77%. This reduction relies on the generation of holograms at high speed. We present software capable of calculating holograms in under 1 ms using a graphics processor unit.

OCIS codes: (140.7010) Laser trapping; (230.6120) Spatial light modulators; (120.4640) Optical instruments; (350.4855) Optical tweezers or optical manipulation.

References and links

1. A. Ashkin, "Accelleration and Trapping of Particles by Radiation Pressure," Phys. Rev. Lett. **24**, 156–159 (1970).
2. D. Grier, "A revolution in optical manipulation," Nat. Photon. **424**, 810–816 (2003).
3. G. Sinclair, P. Jordan, J. Leach, M. Padgett, and J. Cooper, "Defining the trapping limits of holographical optical tweezers," J. Modern Opt. **51**, 409–414 (2004).
4. G. Sinclair, P.Jordan, J.Courtial, M. Padgett, J. Cooper, and Z. Laczik, "Assembly of 3-dimentional structures using programmable holographic optical tweezers," Opt. Express **12**, 5475–5480 (2004).
5. K. D. Wulff, D. G. Cole, and R. L. Clark, "Servo control of an optical trap," Appl. Opt. **46**, 4923–4931 (2007).
6. A. E. Wallin, H. Ojala, E. Haeggstrom, and R. Tuma, "Stiffer optical tweezers through real-time feedback control," Appl. Phys. Lett. **92** (2008).
7. G. Wuite, R. Davenport, A. Rappaport, and C. Bustamante, "An integrated laser trap/flow control video microscope for the study of single biomolecules," Biophys. J **79**, 1155–1167 (2000).
8. M. Wang, H. Yin, R. Landick, J. Gelles, and S. Block, "Stretching DNA with optical tweezers," Biophys. J **72**, 1335–1346 (1997).
9. J. E. Molloy, J. E. Burns, J. Kendrick-jones, R. T. Tregear, and D. C. S. White, "Movement and force produced by a single myosin head," Nature **378**, 209–212 (1995).
10. C. O. Mejean, A. W. Schaefer, E. A. Millman, P. Forscher, and E. R. Dufresne, "Multiplexed force measurements on live cells with holographic optical tweezers," Opt. Express **17**, 6209–6217 (2009).
11. O. Otto, C. Gutsche, F. Kremer, and U. F. Keyser, "Optical tweezers with 2.5 kHz bandwidth video detection for single-colloid electrophoresis," Rev. Sci. Instrum. **79**, 023710 (pages 6) (2008).
12. G. M. Gibson, S. J. Leach, Keen, A. J. Wright, and M. J. Padgett, "Measuring the accuracy of particle position and force in optical tweezers using high-speed video microscopy," Opt. Express **16**, 14,56114,570 (2008).
13. P. J. Rodrigo, L. Gammelgaard, P. Bøggild, I. Perch-Nielsen, and J. Glückstad, "Actuation of microfabricated tools using multiple GPC-based counterpropagating-beam traps," Opt. Express **13**, 6899–6904 (2005).

#118205 - $15.00 USD Received 7 Oct 2009; revised 16 Nov 2009; accepted 18 Nov 2009; published 25 Nov 2009

14. L. Ikin, D. M. Carberry, G. M. Gibson, M. J. Padgett, and M. J. Miles, "Assembly and force measurement with SPM-like probes in holographic optical tweezers," N. J. Phys. **11** (2009).
15. K. Berg-Sorensen and H. Flyvbjerg, "Power spectrum analysis for optical tweezers," Rev. Sci. Instrum. **75**, 594–612 (2004).
16. C. Schmitz, J. Spatz, and J. Curtis, "High-precision steering of multiple holographic optical traps," Opt. Express **13**, 8678–8685 (2005).
17. D. Engström, J. Bengtsson, E. Eriksson, and M. Goksör, "Improved beam steering accuracy of a single beam with a 1D phase-only spatial light modulator," Opt. Express **16**, 18,275–18,287 (2008).
18. T. H. J. Liesener, M. Reicherter and H. J. Tiziani, "Multi-functional optical tweezers using computer-generated holograms," Opt. Commun. **185**, 77–82 (2000).
19. J. Leach, K. Wulff, G. Sinclair, P. Jordan, J. Courtial, L. Thomson, G. Gibson, K. Karunwi, J. Cooper, Z. Laczik, and M. Padgett, "Interactive approach to optical tweezers control," Appl. Opt. **45**, 897–903 (2006).
20. R. D. Leonardo, F. Ianni, and G. Ruocco, "Computer generation of optimal holograms for optical trap arrays," Opt. Express **15**, 1913–1922 (2007).
21. M. Reicherter, S. Zwick, T. Haist, C. Kohler, H. Tiziani, and W. Osten, "Fast digital hologram generation and adaptive force measurement in liquid-crystal-display-based holographic tweezers," Appl. Opt. **45**, 888–896 (2006).
22. URL `http://www.physics.gla.ac.uk/Optics/projects/tweezers/software/`.
23. J. C. Crocker and D. G. Grier, "Methods of Digital Video Microscopy for Colloidal Studies," J. Colloid Interface Scie. **179**, 298–310 (1996).
24. Z. Zhang and C.-H. Menq, "Three-dimensional particle tracking with subnanometer resolution using off-focus images," Appl. Opt. **47**, 2361–2370 (2008).
25. C. Pacoret, R. Bowman, G. Gibson, S. Haliyo, D. Carberry, A. Bergander, S. Régnier, and M. Padgett, "Touching the microworld with force-feedback optical tweezers," Opt. Express **17**, 10,259–10,264 (2009).

1. Introduction

Optical tweezers are a technique by which the user can hold and manipulate micron sized particles for use in a range of experimental procedures. They rely on the optical gradient force created when a tightly focused laser beam is incident on a dielectric particle, pulling it towards the local maxima of intensity [1]. This means that particles can be effectively constrained at a laser focus. Furthermore, by moving the position of the focus the particle may be translated. Holographic optical tweezers (HOT) take this further by using a spatial light modulator (SLM) to dynamically split and control the laser beam [2]. By this method, multiple optical traps may be created and manipulated in arbitrary 3D configurations without time-sharing [3], over tens of microns in the lateral and axial directions [4].

Previously, various techniques have been used to effect feedback control over optically trapped objects and limit the effect of Brownian motion. Most commonly galvanometer-driven mirrors and Acousto-Optic Deflectors (AODs) have been used in conjunction with Quadrant Photodiodes (QPDs) to provide high bandwidth feedback [5, 6]. However, other techniques such as piezoelectric stage control [7] or intensity modulation [8] have also been used. Many such feedback systems are used in biological experiments [9], where position or force feedback control can help prevent damage to biological specimens or increase measurement sensitivity. Until now, most SLMs have updated at video frame rates and had response times of tens of milliseconds, meaning that they are unresponsive at short time-scales. Closed-loop control of HOT has been demonstrated for slowly varying biological forces [10], however the performance of such a system has not been discussed for a bandwidth of more than 0.2Hz.

Recent improvements in the speed of both liquid-crystal based SLMs and modern CMOS camera technology [11, 12] mean that we are able to report holographic optical tweezers that react to a particle's motion in a few milliseconds. Moreover, using a camera allows multiple particles to be tracked, a significant advantage over QPD-based systems. This allows much more sophisticated trap configurations to be used with feedback, for example a tool or probe controlled by multiple traps [13, 14].

#118205 - $15.00 USD Received 7 Oct 2009; revised 16 Nov 2009; accepted 18 Nov 2009; published 25 Nov 2009

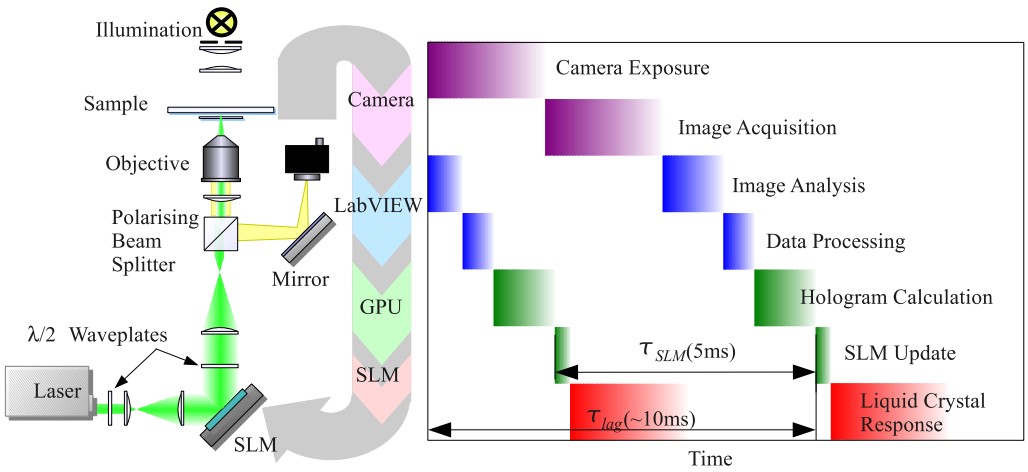

Fig. 1. (a) Experimental setup; a 532nm laser beam is expanded then steered via an SLM onto the back aperture of the microscope objective. This same objective is then used to view the sample with bright-field illumination. The Gantt chart to the right outlines the steps in one iteration of the loop, along with approximate timings and transfer functions used to calculate the theoretical power spectrum in (6).

2. Theory

The motion of a particle in an optical trap is well described by the Langevin equation [15]:

$$m\ddot{x} + \gamma\dot{x} + \kappa x = \zeta(t) \tag{1}$$

where m is the particle's mass (the inertial term $m\ddot{x}$ is usually neglected), $\gamma = 6\pi\eta a$ is the hydrodynamic drag coefficient (for a sphere of radius a in a fluid with viscosity η) and $\zeta(t)$ represents the force exerted on the bead by the thermal motion of the fluid molecules. x is the position of the particle, shown here in one dimension. These equations also hold for y and z independently, as the model used here is separable. The restoring force from the optical trap is characterised by the spring constant κ, which assumes a Hookean optical trap at $x = 0$. By taking the Fourier transform of (1) and using the fluctuation-dissipation theorem to give the power spectrum of ζ as $\gamma k_B T/\pi$, where k_B is Boltzmann's constant and T is absolute temperature, we can derive the power spectrum of x for a particle held in a stationary trap as

$$(-\omega^2 m + \mathrm{i}\gamma + \kappa)\tilde{x} = \tilde{\zeta}(\omega) \tag{2}$$

$$S_x = \gamma k_B T/\pi \left((\kappa - m\omega^2)^2 + \gamma^2\omega^2\right)^{-1} \tag{3}$$

where $\tilde{x}$ denotes the Fourier transform of x and S_x is its power spectrum. We can modify (1) to include a varying trap position in the restoring force term:

$$m\ddot{x} + \gamma\dot{x} + \kappa\left(x - x_{\mathrm{trap}}(t)\right) = \zeta(t). \tag{4}$$

If, x_{trap} were simply proportional to $-x$, the only effect of feedback would be to increase the effective stiffness of the trap $k_B T/\langle x^2\rangle$. However, each element of the feedback system (outlined in Fig. 1) introduces latency and filtering. The SLM refreshes at discrete intervals, which gives rise to low pass filtering (transfer function $\mathrm{sinc}(\omega\tau_{\mathrm{SLM}}/2)$) and an effective latency of half the update period $\tau_{\mathrm{SLM}} = 5\,\mathrm{ms}$ (transfer function $\exp(-\mathrm{i}\omega\tau_{\mathrm{SLM}}/2)$). Aliasing can be neglected

#118205 - $15.00 USD Received 7 Oct 2009; revised 16 Nov 2009; accepted 18 Nov 2009; published 25 Nov 2009

both as the power spectrum falls sharply with ω and the low pass filtering from the SLM acts as an antialiasing filter. The liquid crystal also has a finite response time $\tau_r \approx 2\,\mathrm{ms}$, modelled by the transfer function $1/(1+\mathrm{i}\tau_r\omega)$, and additional latency in the system (due to software and image acquisition) is represented by transfer function $\exp(\mathrm{i}\omega\tau_{\mathrm{lag}})$. This leads to an expression for $\tilde{x}_{\mathrm{trap}}$ of

$$\tilde{x}_{\mathrm{trap}} \approx -G\tilde{x}\,\mathrm{sinc}\,(\omega/\tau_{\mathrm{SLM}}/2)\,e^{-\mathrm{i}\omega(\tau_{\mathrm{SLM}}/2+\tau_{\mathrm{lag}})}\frac{1}{1+\mathrm{i}\tau_r\omega} \tag{5}$$

where G is the feedback gain. Substituting (5) into (2), we can derive the power spectrum for a bead in a closed loop holographic trap:

$$S_x = \gamma k_B T/\pi \left| -\omega^2 m + \mathrm{i}\gamma\omega + \kappa + \kappa G\,\mathrm{sinc}\,(\pi\omega/\omega_{\mathrm{SLM}})\,e^{-\mathrm{i}\omega(\tau_{\mathrm{SLM}}/2+\tau_{\mathrm{lag}})}/(1+\mathrm{i}\tau_R\omega)\right|^{-2} \tag{6}$$

Due to the approximation made in (5) that aliasing in the feedback signal is unimportant, this result is only valid for cases where the update frequency of the SLM is much greater than the corner frequency of the trap; with currently available technology this restricts us to relatively weak traps or highly viscous fluids. Figure 3 shows this spectrum plotted along with experimental data for a 5μm bead in a trap with $\kappa = 2.1\times10^{-6}\mathrm{Nm}^{-1}$. The spectra exhibit the expected suppression of Brownian motion at low frequencies (decreasing the variance by a factor of $1+G$), but have a resonance at a frequency of approximately $(2\tau_{\mathrm{SLM}}+4\tau_{\mathrm{lag}}+2\tau_r)^{-1}$. Control theory establishes it is impossible to achieve a broadband reduction in the system's sensitivity to error, and hence this resonance cannot be eliminated [5]. However, as the underlying power spectrum for $G=0$ has a Lorentzian shape, the impact of the resonance on the particle's position distribution decreases as it is moved to higher frequencies; thus the improvement in effective trap stiffness depends to a large extent on minimising latency in the system.

To obtain the expected improvement in spatial localisation, we can calculate the variance of the particle's position distribution $\langle x^2\rangle$ (and similarly $\langle y^2\rangle$) by numerically integrating the power spectrum. For a standard 60Hz SLM, we would not expect a significant reduction in $\langle x^2\rangle$. However, with an SLM running at 203Hz the improvement could be as much as 50%. The improvement for a 5μm bead in a relatively weak holographic trap ($\kappa \approx 2.1\times10^{-6}\,\mathrm{Nm}^{-1}$) is shown in the inset in Fig. 3 along with experimental data, as a function of $\tilde{f}(\omega)$ which is assumed to be a constant. It shows a reduction in $\langle x^2\rangle$ as gain is increased, which reaches a minimum and starts to increase again. At higher gains, the assumption in (4) that the restoring force is unlimited becomes invalid, as the trapping force falls off once $|x-x_{\mathrm{trap}}| \gtrapprox a$. In practice this means the bead is lost from the trap.

3. Experimental setup

As outlined in Fig. 1, the trapping beam is generated by a 532nm frequency doubled Nd:YAG laser (Laser Quantum Opus), operating at an output power of 1 Watt). The beam's polarisation is controlled via $\lambda/2$ waveplates to maximise diffraction efficiency. The beam is expanded and directed onto a Boulder Nonlinear Systems Spatial Light Modulator (XY Series) 512x512 pixels, operating at 203Hz, 16 bit. The high bit depth means the trap can be steered to a theoretical accuracy of better than 1$\mathring{A}$ [16, 17], and the diffraction efficiency varies by less than 10% over the $20\,\mu$m field of view used here. The diffracted beam is then sent via a polarising beam splitter cube into an inverted Zeiss Microscope (Axiovert 200). The same objective lens (Zeiss 100X Plan-Neofluar, NA 1.30) was used for trapping and imaging the particles onto a Prosilica GC640 Gigabit Ethernet camera. The frame rate of this camera depends on the field of view, for example a single bead can be imaged at over 1 kHz and a triangular configuration of beads side $14\,\mu$m across could be imaged at 460 Hz. The images were analysed on-line using a centre

#118205 - $15.00 USD Received 7 Oct 2009; revised 16 Nov 2009; accepted 18 Nov 2009; published 25 Nov 2009

of mass algorithm. Image analysis and feedback control were performed in LabVIEW running on a quad core computer, which also contained the graphics processor used for hologram calculation (nVidia Quadro FX 5600).

4. Hologram calculation

After tracking with the camera the measured particle positions were used to calculate the new trap positions.

$$x_{\text{trap}} = -Gx \tag{7}$$

In order to minimise latency, the resulting holograms were calculated with a non-iterative algorithm based on direct superposition of wedges and lenses [18, 19] running on the system's graphics processor.

To calculate a hologram which will produce multiple diffraction-limited spots, we use an analytic expression for one spot, the combination of a lens and a prism:

$$\phi_i(x,y) = k_x x + k_y y + k_z(x^2+y^2). \tag{8}$$

We then superpose these holograms to get the final phase-only hologram $\phi_T(x,y)$:

$$\phi_T = \text{Arg}\left[\sum_i \exp\left(\text{i}\phi_i(x,y)\right)\right] = \text{Arg}\left[\sum_i \exp\left(\text{i}[k_x x + k_y y + k_z(x^2+y^2)]\right)\right] \tag{9}$$

Iterative algorithms are often used to optimise the hologram, which is particularly important for large arrays of spots [20]. However, in our case the high speed outweighs the imperfections in the holograms produced.

Driven by the demand for realistic 3D graphics, modern GPUs have a large number of processing cores (128 for the Quadro FX 5600), which can execute custom "shader programs" during rendering. This has previously been used to calculate $\phi_i(x,y)$ as arrays and then to sum the arrays [21]. However we have used one custom shader to allow the entire algorithm to be executed in parallel. We evaluate (9) using a loop over i for each pixel to eliminate the need for large arrays. The consequent reduction in memory access gives an order of magnitude increase in speed. The OpenGL environment allows the hologram to be rendered directly into the frame buffer in a single pass. This is a significant advantage over nVidia's more flexible CUDA environment where the hologram must be calculated as a large array then re-rendered from texture memory to the frame buffer. Our algorithm takes less than a millisecond to calculate and display a hologram, allowing us to achieve sufficiently low latencies to make feedback viable. This can be freely downloaded from [22].

5. Results and discussion

It is important to distinguish the addressing rate of the SLM and the speed with which a beam can be steered in practice. To measure the beam steering speed of the SLM, it was used to switch the laser spot between two positions repeatedly. The intensity at these two positions was measured using the camera at a frame rate of 1.6 kHz and is plotted in Fig. 2. This shows the response to a 50 Hz square wave, and is close to the exponential approximation in Section 2 with a response time $\tau_{\text{R}} \approx 2$ ms. The asymmetry in the response may be due to nonlinearities in the camera's response and the overall decrease in diffraction efficiency as the SLM switches from one hologram to the next.

The power spectra of a single bead's fluctuations about the target position are shown in Fig. 3 for various values of feedback gain G. The trap had a stiffness of $\kappa = 2.1 \times 10^{-6}\,\text{Nm}^{-1}$, measured by fitting a Lorentzian to the power spectrum in the case of no feedback. This had

#118205 - $15.00 USD Received 7 Oct 2009; revised 16 Nov 2009; accepted 18 Nov 2009; published 25 Nov 2009

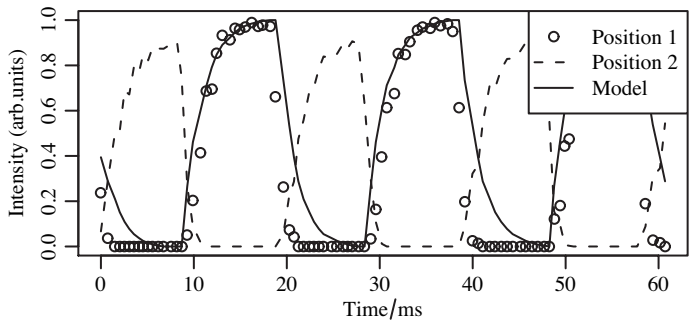

Fig. 2. Intensity at two points, when the SLM is used to switch the laser spot between them. The solid line shows the modelled response of Section 2, with $\tau_R = 2\,\mathrm{ms}$.

a corner frequency $f_c = \kappa/(2\pi\gamma) \approx 4.0\,\mathrm{Hz}$. The response time was taken as 2ms to match the experimentally observed response of the SLM. This left additional latency as the only parameter to fit; the best fit value was 10ms (see Fig. 1). An excellent agreement is seen for low feedback gains, though at higher gains the resonance is less sharp than predicted. This discrepancy is perhaps due to the finite trap depth as discussed above. However, the system still performs as expected, reducing $\langle x^2 \rangle$ by 44% corresponding to an increase in effective trap strength $\kappa' = k_B T / \langle x^2 \rangle$ of 77%. The data shown in Fig. 3 were collected with the high speed camera running at 1kHz. The exposure time was close to 1ms, which acted as an antialiasing filter. The deviation from the Lorentzian line at high frequencies arises from the noise floor of the camera system, however its contribution to $\langle x^2 \rangle$ is extremely small.

The results in Fig. 3 are for a single particle, and could be reproduced with other techniques such as AODs. The advantage of holographic optical tweezers is that we can easily extend this to multiple particles, and to that end Fig. 4 shows three trapped beads and histograms of their displacements from the trap centres (x and y). The variance of their position distributions was reduced by 47% on average when position-clamping was turned on. This demonstrates the unique ability of holographic optical tweezers and camera-based position measurement to perform feedback on multiple optical traps. In the intrests of experimental simplicity we use only a proportional control in the generation of all feedback signals, no integral or derivative gain was used. The power spectra for three beads are also shown in Fig. 4(c), for no feedback and for the optimal gain $G = 1.7$. This optimal value was chosen by analysing a number of experimental data sets over a wide range of gain values and finding the minimum varience in position (see 3 (inset)).

These power spectra are very similar to those shown in. Fig. 3, for a single particle. This is in spite of the fact that the larger region of interest (260 x 210 pixels) necessitated a slower frame rate for the camera of 460 Hz (c.f. 1 kHz). This shows the slower frame rate does not significantly affect the system's performance, only the range over which power spectra can be plotted. The resonance at approximately 100 Hz we believe stems from modulation of the intensity of the illumination, and misalignments in the microscope condenser. The peak is present even when no control is used and its height is uncorrelated with gain.It accounted for $\lessapprox 5\%$ of the variances. Filtering out the resonance gives a slightly greater improvement (by a few percent) in $\langle x^2 \rangle$. Other configurations of beads, such as a line, were also used and similar results were obtained.

Two potential concerns in the use of SLMs for closed-loop HOT are the discrete nature of the SLM and imperfections resulting from the simple hologram design method used. The former can result in the trap being constrained to certain discrete positions due to the finite

#118205 - $15.00 USD Received 7 Oct 2009; revised 16 Nov 2009; accepted 18 Nov 2009; published 25 Nov 2009

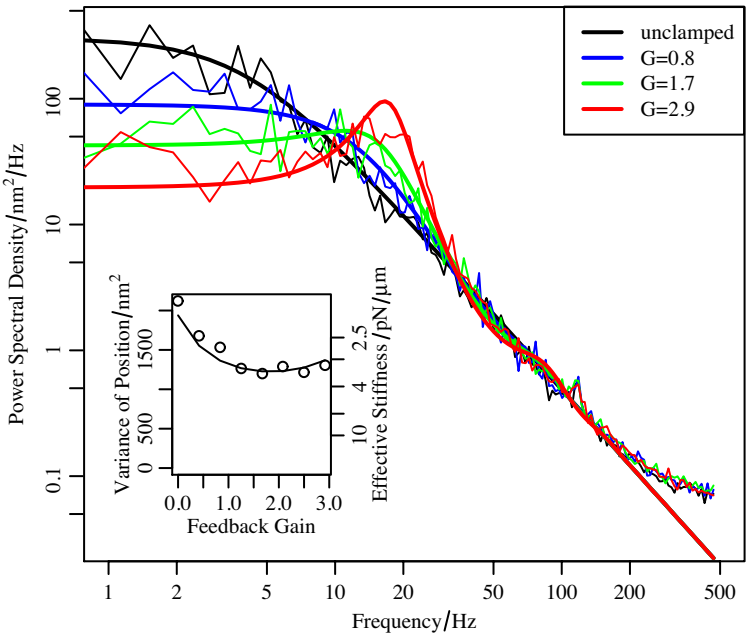

Fig. 3. Experimentally measured power spectra (points) and theoretical curves (lines) from (6) for a 5μm bead in a trap with stiffness $\kappa \approx 2.1 \times 10^{-6}\mathrm{Nm}^{-1}$. [inset] The variance of the particle's position as a function of feedback gain, with experimental data as points and the theoretical curve as a line. Model parameters and experimental data are the same for both plots.

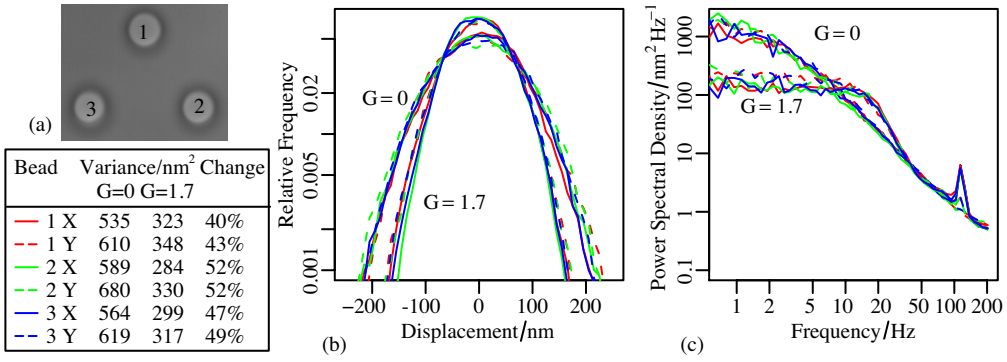

Bead	Variance/nm^2 G=0	Variance/nm^2 G=1.7	Change
1 X	535	323	40%
1 Y	610	348	43%
2 X	589	284	52%
2 Y	680	330	52%
3 X	564	299	47%
3 Y	619	317	49%

Fig. 4. Three 5μm beads in optical traps (a), along with a histogram of the position distributions (b) and the power spectra of their motion (c) for no gain and a gain of 1.7. The variances with and without clamping, and the percentage decrease in $\langle x^2 \rangle$ and $\langle y^2 \rangle$ are shown in the legend.

#118205 - $15.00 USD Received 7 Oct 2009; revised 16 Nov 2009; accepted 18 Nov 2009; published 25 Nov 2009

resolution and number of gray levels on the SLM [16, 17]. The Boulder SLM used for this experiment uses 16-bit values which, even after processing, means there are several thousand usable gray levels and the theoretical step size is far below 1$\mathring{A}$. This is much smaller than the size of the Brownian motion we seek to suppress. The second concern, that of non-uniform trap intensities or coupling between traps, is primarily an issue for large, regular arrays of traps rather than the small number of traps used here. More sophisticated algorithms could be used to mitigate this effect should the technique be applied to large arrays [20]. Despite both these concerns, the agreement of our system's performance with the theoretical model shows that neither concern is the limiting factor. Rather, it is latency in the control loop which limits the system's performance.

6. Conclusions

We present a closed-loop holographic optical tweezers system capable of feedback on multiple particles in 3 dimensions without the need for time sharing or complex optics. We find good agreement between experimentally measured results and our theoretical model, and reduce the variance of a 5μm bead's position by 44%. The holographic position-clamp does not have the high bandwidth of AOD or galvo-mirror based systems, however its ability to clamp multiple particles makes it a promising technique. Furthermore, its bandwidth (and hence the improvement in localisation) will improve as SLM technology develops further. It is also possible to use a camera to estimate a bead's axial position [23, 24] and future work could use this, combined with the 3D capabilities of HOT, to position clamp in 3D. As with AODs, closed-loop operation can combine highly sensitive force measurement with good spatial localisation. It therefore has many exciting applications to micro-tools [13, 14] or force-feedback interfaces [25].

#118205 - $15.00 USD Received 7 Oct 2009; revised 16 Nov 2009; accepted 18 Nov 2009; published 25 Nov 2009